

## REFINING OF METALLURGICAL SILICON FOR CRYSTALLINE SOLAR CELLS

E. Fourmond, C. Ndzogha, D. Pelletier, Y. Delannoy, C. Trassy,  
CNRS EPM (UPR 9033), 1340 rue de la piscine, 38402 Saint martin d'Hères cedex, France  
Christian.Trassy@grenoble.cnrs.fr

Y. Caratini, Y. Baluais,  
INVENSIL, 517, av. de La Boisse, 73025 Chambéry Cedex, France

R. Einhaus,  
APOLLON SOLAR, 2 rue Dulong, 75017 PARIS, France

S. Martinuzzi, I. Périchaud  
TECSEN (UMR 6122), Fac. Sci. & Tech. Univ. d'Aix-Marseille III, 13997 Marseille Cedex 20, France

**ABSTRACT:** A plasma-refining technique is applied to upgraded metallurgical grade silicon (UMG) to produce solar grade silicon for multi-c silicon ingots at direct costs lower than 15€/kg. Using oxygen and hydrogen as reactive gases injected in the plasma, boron is removed from the material mainly in form of BOH and BO. The boron volatilization time has been reduced to 50 min compared to previous processes, by increasing the temperature of the silicon bath. At the same time, the Al, Ca, C, O concentrations are strongly reduced. From a first batch of purified UMG Silicon, multi-crystalline ingots (12kg), wafers (125x125mm<sup>2</sup>) and solar cells have been produced for an evaluation of this intermediate material. The obtained solar cells gave efficiencies of up to 11.7%. Process development towards an up-scaled pilot equipment is on the way to further increase the purification efficiency.

**Keywords:** Silicon, Metallurgical-Grade, PV Materials.

### 1 INTRODUCTION

More than 90% of today's PV modules on the market are made from crystalline silicon solar cells and more than 50% of these solar cells are produced on multi-crystalline silicon wafers, the remaining part accounts for mono-crystalline silicon wafers and multi-crystalline ribbons.

At the same time the world-wide production of PV modules has been rising continuously by at least 33% per year (between 1998 and 2003). These high growth rates directly result in an increasing demand for silicon feedstock, which is the raw material for the production of silicon wafers. Since the classical sources of silicon feedstock for the PV industry – silicon waste from the production of electronic grade silicon as well as silicon rejects, off-spec material from the microelectronic industry – are limited in quantity, a serious shortage of supply of raw material for the PV industry arises, as for example analyzed in detail in [1], leading to increasing production costs for crystalline silicon based PV modules.

This paper presents intermediate results of an approach to produce solar grade silicon by refining upgraded metallurgical silicon (UMG-Si) from INVENSIL to a level below the high purity electronic grade quality, but with a sufficiently high quality for solar cell processing. The final objective of this work is to arrive at an industrially exploitable process to directly produce multi-crystalline Si ingots by means of an innovative, integrated purification/crystallization process, at direct production costs below 15 €/kg at ingot level.

The presented silicon purification technology is in parts based on fundamental development work, already carried out in the frame of the European ARTIST project [2], focusing on the technological progress that has been achieved since the end of this project.

### 2 PROCESS DESIGN

#### 2.1 Purification technique

The purification of metallurgical grade silicon by plasma has been studied by several groups [3, 4]. The principle consists in the use of plasma gas containing oxidizing species, drawn on the surface of liquid silicon. This leads silicon impurities to react with reactive gases and create volatile species. Among silicon impurities, Boron is of relevant importance concerning the photovoltaic quality of the silicon. Due to its poor segregation coefficient ( $k=0.85$ ) it cannot be removed by directional solidification. Plasma purification technique seems to be a promising technique to decrease boron content before directional solidification. As previously described [5], boron with addition of oxygen and hydrogen will evaporate mainly in the form of BOH and BO.

#### 2.2 Experimental setup

The pilot consists in an inductive plasma torch combined with an inductive cold crucible (figure 1). The process takes place in an atmosphere-controlled, water-cooled chamber.

The plasma torch is made of three concentric tubes. The axial tube (injector) is used to inject reactive gases mixed with argon into the plasma. The plasma gas (argon) is introduced between the outer and the intermediate tube. The flow rates are 70 l/min for plasma gas, 4 l/min for auxiliary gas, and 2.5 l/min for injection. The plasma power is 30 kW, and the induction frequency is 3.4 MHz. The distance between the plasma torch and the crucible is 4 cm.

The cold crucible is constituted by several water cooled sectors made of copper. The capacity can vary between 3 kg (120 mm inner diameter) and 10 kg (200 mm i.d.). The induction frequency varies from 7 to 12 kHz, depending on the size of the crucible and the amount of silicon. This range of frequency leads to a strong stirring of the liquid phase during the process, as

previously described [6]. The induction power ranges from 50 to 110 kW.

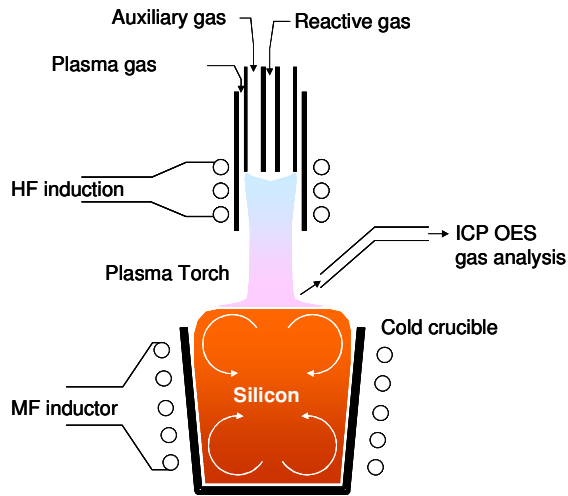


**Figure 1:** Schematic diagram of the apparatus.

During the run the pressure is stabilized slightly above the atmospheric pressure by means of an automatic valve. The flue gases are sampled at the outlet of the chamber, and carried back to an analytical inductively coupled plasma to be analyzed by optical emission spectroscopy (ICP-OES). It is thus possible to monitor the concentrations of elemental impurities in the flue gases, and to correlate them with the decrease of impurity content in the liquid silicon during the process.

### 2.3 Process description

The complete process consists in several stages. We must first note that the electromagnetic field frequency used with the cold crucible does not allow direct fusion of the silicon, since the skin depth for silicon at room temperature is around 150 mm. The fusion of the silicon is thus initiated by the plasma torch. When the volume of the liquid phase at the top of the crucible increases sufficiently the induction power takes over. The resistivity of the liquid silicon is below  $10^{-4} \Omega \cdot \text{cm}$ , which corresponds to a skin depth of 5 mm.



**Figure 2:** Liquid silicon dome under plasma.

The second step consists in the refilling of the liquid bath by injecting silicon powder through the axial tube of the plasma torch. When the entire solid silicon is melted and the level of the liquid reaches the desired height, the purification step begins (figure 2). Oxygen and hydrogen are injected through the axial tube, at a flow rate of 0.5 and 2.5 l/min, respectively. The purification time is controlled by monitoring the B/Si ratio in the flue gases by

ICP-OES. The last step of the process is the cooling and solidification of the silicon. Proper directional crystallization is not aimed at this step. The resistivity of the ingot is measured afterwards, and chemical analyses of the impurity concentration are carried out.

### 3 SILICON TEMPERATURE INFLUENCE ON THE PURIFICATION TIME

Previous thermodynamics studies [5] have reported that the removal of the boron from the liquid silicon follow a first order rule. The boron content decreases exponentially with the treatment duration. The time constant extracted from the decrease rate describes the efficiency of the process. This time corresponds to the moment when 64% of the impurity has been volatilized.

We have studied the influence of the temperature of the liquid silicon on the time constant of the purification. By adjusting the power applied to the cold crucible we can increase the temperature of the bath. Figure 3 shows the B/Si ratio curves obtained from the ICP-OES signal of the flue gases in two different cases. The decrease in the B/Si intensity ratio follows an exponential law. The temperature difference between the two cases was about  $150^\circ\text{C}$ . Absolute temperature measurements are not precise, mainly due to the plasma emissivity; but the evaluation of the change in temperature is relatively precise ( $\pm 20 \text{ K}$ ). The only change in parameters between the two runs was the crucible induction power.

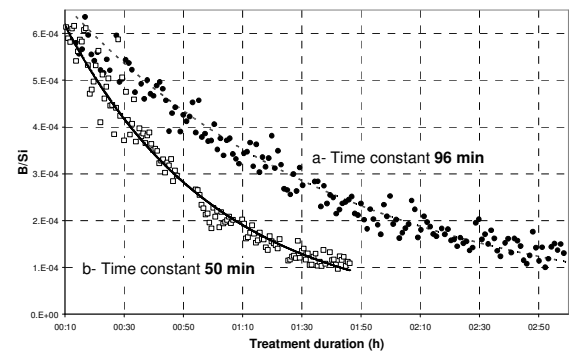


**Figure 3:** B/Si ratio in flue gases as a function of time. The silicon temperature difference between case a and b is  $150^\circ\text{C}$ .

The increase of the liquid temperature has two major effects on the volatilization process. First of all, we can verify the previous thermodynamics statement [5] that boron volatilization increases with higher silicon temperature. As a result the time constant decreases from 96 to 50 min. Secondly, it allows the use of higher oxygen content in reactive gases. The formation of a silica layer on the surface of the liquid, due to oxygen injection, is indeed a limiting phenomenon in the volatilization process. As simulated on figure 4, this silica layer subsists at higher temperature when oxygen content increases. Overheating the silicon allows us to employ higher oxygen in the reactive gases without the formation of silica. It has been thus possible to use up to 1.35 l/min of  $\text{O}_2$  in case b, instead of 0.63 l/min max. in case a.

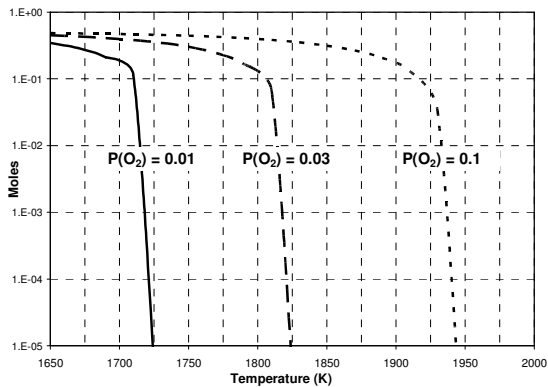


**Figure 4:** Effect of oxygen partial pressure  $P(O_2)$  in plasma gases on the amount of silica. Silica volatilizes at higher temperature when  $P(O_2)$  increases.

#### 4 EVALUATION OF REFINED SILICON

In order to evaluate the quality of the silicon obtained after plasma processing, around 50 kg of refined silicon were produced with the aim to produce standard multi-crystalline silicon wafers for analysis purposes and for the processing of standard solar cells.

##### 4.1 Ingot crystallization and characterization

Purified silicon was used as feedstock for the production of two test ingots of 12 kg. These ingots were crystallized using a state-of-the-art directional solidification process. The obtained ingots were crack free and showed large columnar grains, indicating already that there were no material related problems during the crystallization itself. The dislocation density is lower than  $10^4 \text{ cm}^{-2}$ . Figure 5 shows a photograph of a perpendicular slice which was cut from one of the ingot.

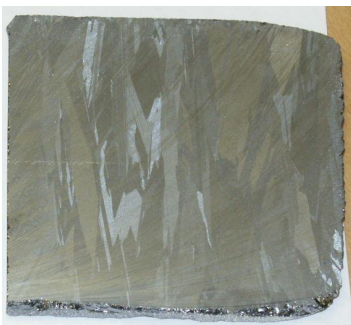


**Figure 5:** Perpendicular slice of a multi-crystalline ingot produced from plasma purified metallurgical silicon.

The multi-c silicon ingots were cut into square shaped blocks and a first characterization by four-point-probe was carried out to determine the resistivity of the ingot. Figure 6 shows the resistivity profile obtained from the bottom of the ingot to the top. Compared to an ingot produced from purified silicon of the ARTIST project whose resistivity profile is also shown in figure 6, the resistivity could be increased to values up to  $0.5 \Omega\text{cm}$  in the upper part of the recent ingots. This could be due to the weak difference of segregation coefficient between boron and phosphorous, leading to a strong change in the compensation effect. Both ingots were p-type.

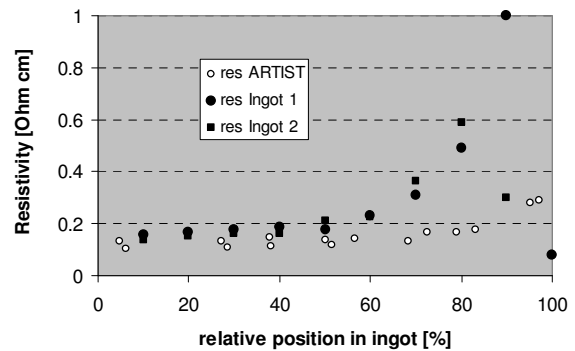


**Figure 6:** Resistivity profiles of the multi-c ingots made from plasma purified silicon (Ingot 1 & 2) compared to the resistivity of an ingot produced during the ARTIST project.

The obtained blocks were cut in  $125 \times 125 \text{ mm}^2$  wafer of  $300 \mu\text{m}$  thickness by a standard multiple wire sawing process. These wafers were chemically analyzed for impurity concentrations by ICP and IR absorption. The obtained impurity concentrations for wafers from the middle of the ingot are summarized in Table 1.

**Table 1:** Ingot impurities concentrations in  $\text{ppm}_w$ . Some impurity concentrations (Fe) are below the detection limits.

Ingot	B	P	O	C	Fe	Ca
Ingot I	3.5	3	940	290	<10	<10
Ingot II	3.5	3.5	840	290	<10	12.5

Comparing the dopant concentrations and the measured resistivities, two phenomena can be assumed: compensation effects, and dopant passivation under complex forms, like phosphates or borides, which are electrically not active and stable at high temperatures. These complexes are most probably formed during the high temperature plasma treatment. However, solar cells made from these wafers exhibit no degradation after light soaking tests (24 hours after storage in the dark), contrary to the results obtained in the frame of the ARTIST project. The total absolute concentration of doping atoms is in the order of than  $10^{16} \text{ cm}^{-3}$  to  $10^{17} \text{ cm}^{-3}$ . Standard multi-c silicon wafers for photovoltaic applications with a resistivity of  $1 \Omega\text{cm}$  have a doping concentration at the lower range of  $10^{16} \text{ cm}^{-3}$ .

The O and C concentrations are still two orders of magnitude too high and risk to degrade the photovoltaic performance of the material. Modifications on the upstream processing stages, during the production of the UMG silicon are currently under investigation in order to further reduce the O and C concentration of the starting material. The intra-grain oxygen concentration is in the range of 1-10 weight ppm.

An analysis of the wafers by LBIC exhibit a relatively low average diffusion length, between 20 and  $30 \mu\text{m}$ , see also the photocurrent cartography in figure 7. However, no important contrast between grains and grain boundaries is visible. Reasons for the low diffusion length are certainly the remaining, relatively high dopant concentrations, as well as the residual oxygen and carbon.

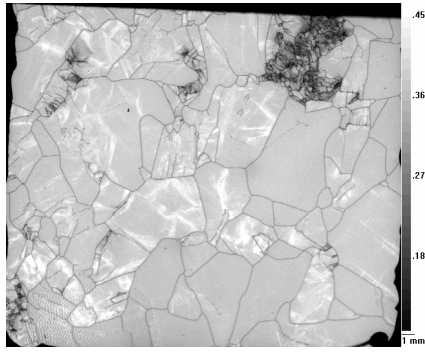


**Figure 7:** LBIC cartography of a wafer. The white zones on the map correspond to diffusion lengths larger than 120-150  $\mu\text{m}$ .

QSSPC characterisation at an injection level of  $5 \cdot 10^{14} \text{ cm}^{-3}$  of different wafers at ISE gave a minority carrier lifetime between 0.3  $\mu\text{s}$  and 1.0  $\mu\text{s}$ .

#### 4.2 Solar cells results

A representative number of the obtained multi-c Silicon wafers from both ingots have been selected to process solar cells, in order to get an idea about the photovoltaic performance of the material. The solar cells have been processed with an industrial type standard process at Fraunhofer ISE. The process steps were: saw damage removal (20  $\mu\text{m}$  from each surface),  $\text{POCl}_3$  diffusion resulting in an emitter of  $40 \Omega/\text{sq}$ , ARC coating with sputtered SiN, screen printed metallization on front and rear surface and co-firing of contacts. The IV characteristics of the best solar cells obtained are shown in Table 2. The major difference compared to standard solar cells is the low  $I_{sc}$  which is related to the remaining relatively high residual concentration of impurities and related recombination effects, which are also visible in the low lifetimes. The low resistivity of the wafers gives rise to the high  $V_{oc}$ , which is by itself comparable to standard multi-c solar cells. The fill factor is also comparable to standard multi-c solar cells. The lower than standard efficiencies are therefore mainly due to the low  $I_{sc}$ . The distribution of the conversion efficiency with respect to the ingot position is shown in figure 8. The degradation of the efficiency at the top of the ingot is related to the strong compensation effect which degrades the minority carrier lifetime.

**Table 2:** Best solar cells results.

Ingot	$V_{oc}$ (mV)	$I_{sc}$ (mA/cm <sup>2</sup> )	FF	$\eta$ (%)
1	610.6	24.13	0.768	11.3
2	612.0	25.10	0.763	11.7

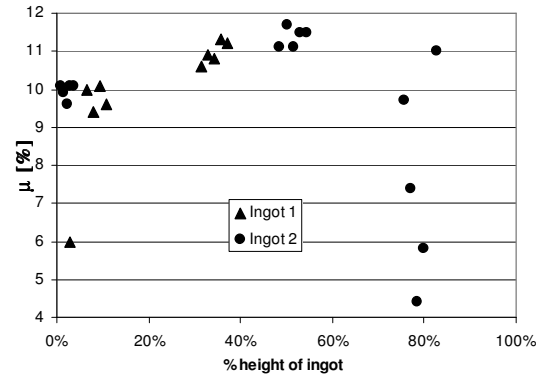


**Figure 8:** Cell efficiency distribution among ingots.

## 5 CONCLUSION

The obtained results of plasma purification of UMG silicon are promising, since the purification time has been reduced comparing to the previous results of the ARTIST project. 11.7% solar cells efficiency on intermediate purified multi-c silicon have been achieved. By now, the maximum equipment capacity at a laboratory scale has been reached. For further process development towards an industrial process a semi-industrial scale pilot equipment with a capacity of 40-50kg is foreseen.

## 6 ACKNOWLEDGEMENTS

Authors would like to thank SINTEF for ingot crystallization, Fraunhofer ISE for solar cells processing and measurements, and Service Central d'Analyse du CNRS (UPS 59, Vernaison) for chemical analysis.

## 7 REFERENCES

- [1] P. Woditsch and W. Koch, *Solar grade silicon feedstock supply for PV industry*, Solar Energy Materials & Solar Cells 72 (2002), pp. 11 – 26.
- [2] R. Einhaus et al., *Purification of low quality silicon feedstock*. Proceedings of the 28<sup>th</sup> IEEE PVSEC, Anchorage, USA (September 2000) pp. 221-224.
- [3] N. Yuge et al., *Purification of Metallurgical-Grade Silicon up to Solar Grade*, Progr. Photovoltaics: Res. Appl. 9 (2001), pp. 203-209.
- [4] J. Erin, D. Morvan, J. Amouroux, *Optimisation des conditions de fonctionnement d'un pilote plasma de 25 kW pour la purification de silicium*, J. Phys. III France 5 (1995), pp. 585-604.
- [5] C. Alemany et al., *Refining of metallurgical-grade silicon by inductive plasma*, Solar En. Mat. and Solar Cells 72 (2002), pp. 41-48.
- [6] Y. Delannoy et al., *Plasma-refining process to provide solar-grade silicon*, Solar En. Mat. and Solar Cells 72 (2002), pp. 69-75.